https://doi.org/10.5194/acp-2021-439
Preprint. Discussion started: 18 June 2021
© Author(s) 2021. CC BY 4.0 License.

Atmospheric Chemistry and Physics Discussions

Improved gridded ammonia emission inventory in China

Baojie Li[1], Lei Chen[1], Weishou Shen[1], Jianbing Jin[1], Teng Wang[2], Pinya Wang[1], Yang Yang[1], and Hong Liao[1]*

[1] Jiangsu Key Laboratory of Atmospheric Environment Monitoring and Pollution Control, Jiangsu Collaborative Innovation Center of Atmospheric Environment and Equipment Technology, School of Environmental Science and Engineering, Nanjing University of Information Science and Technology, Nanjing, 210044, China
[2] College of Oceanography, Hohai University, Nanjing, 210098, China

Correspondence to: Hong Liao (hongliao@nuist.edu.cn)

Abstract. As a major alkaline gas in the atmosphere, NH_3 significantly impacts atmospheric chemistry, ecological environment, and biodiversity. Gridded NH_3 emission inventories can significantly affect the accuracy of model concentrations and play a crucial role in the refinement of mitigation strategies. However, several uncertainties are still associated with existing NH_3 emission inventories in China. Therefore, in this study, we focused on improving fertilizer application-related NH_3 emission inventories. We comprehensively evaluated the dates and times of fertilizer application to the major crops that are cultivated in China, improved the spatial allocation methods for NH_3 emissions from croplands with different rice types, and established a gridded NH_3 emission inventory for mainland China with a resolution of 5 min × 5 min in 2016. The results showed that the atmospheric NH_3 emissions in mainland China amounted to 12.11 Tg, with livestock waste (44.8%) and fertilizer application (38.6%) being the two main NH_3 emission sources in China. Obvious spatial differences in NH_3 emissions were also observed, and high emissions were predominantly concentrated in North China. Further, NH_3 emissions tended to be high in summer and low in winter, and the ratio for the July–January period was 3.08. Furthermore, maize and rice fertilization in summer was primarily responsible for the increase in NH_3 emissions in China, and the evaluation of the spatial and temporal accuracy of the NH_3 emission inventory established in this study using the WRF-Chem and ground station- and satellite-based observations showed that it was more accurate than other inventories.

1 Introduction

Ammonia, a major form of reactive nitrogen, plays an important role in atmospheric chemistry, ecological environment, and biodiversity (Sheppard et al., 2011; Zhang et al., 2018). As the major alkaline gas in the atmosphere, it can form $(NH_4)_2SO_4$ and NH_4NO_3 with H_2SO_4 and HNO_3 produced from the oxidation of SO_2 and NO_x, respectively, and contribute to the formation of secondary inorganic aerosols (SIA), thereby increasing the concentration of $PM_{2.5}$ (Fu et al., 2017). For example, in China, the contribution of agriculture-related NH_3 emissions to SIA and $PM_{2.5}$ is 29 and 16%, respectively (Han et al., 2020), and recent studies have shown that NH_3 can also react with alkanes in the atmosphere to form toxic organic species, including

https://doi.org/10.5194/acp-2021-439
Preprint. Discussion started: 18 June 2021
© Author(s) 2021. CC BY 4.0 License.
Atmospheric Chemistry and Physics Discussions

methylamine (CH_3NH_2), dimethylamine (C_2H_7N), and trimethylamine (C_3H_9N), which are harmful to organisms (You et al., 2014).

Additionally, especially in eastern China, haze pollution has been frequently observed and is characterized by an extremely high concentration of $PM_{2.5}$, with a remarkably high proportion (20−60%) of SIAs, (Ding et al., 2016; Elser et al., 2016; Wang et al., 2016). The Chinese government has taken effective measures to control SO_2 and NO_X emissions, and a large number of studies have indicated that SO_2 and NO_X concentrations and emissions have decreased in recent years (Zheng et al., 2018; Li et al., 2019b; Zhang et al., 2019). However, measures to reduce NH_3 emissions are limited. Satellite retrievals have shown an increase in NH_3 vertical column densities (VCDs) in recent years (Warner et al., 2017; Chen et al., 2020), and China has become a global "hotspot" for NH_3 emissions and NH_3 pollution (Liu et al., 2013; Liu et al., 2019a). Such increases in NH_3 concentrations may reduce the effectiveness of particle pollution control achieved via SO_2 and NO_X emission reduction (Wang et al., 2013; Fu et al., 2017). Therefore, to effectively control PM pollution and reduce SIA concentrations in China, strategies to reduce NH_3 emissions are urgently required.

Recently, NH_3 emission reduction has been proposed as a strategic option for mitigating haze pollution (Liu et al., 2019b). Several organizations and researchers have established gridded NH_3 emission inventories, such as the MEIC, PKU-NH_3, MASAGE_NH_3, EDGAR, and REAS (Streets et al., 2003; Paulot et al., 2014; Fu et al., 2015; Kang et al., 2016; Li et al., 2017; Zhang et al., 2017; Zhang et al., 2018; Crippa et al., 2020; Kurokawa and Ohara, 2020). Based on these studies, substantial progress has been made in the development of NH_3 emission inventories. However, NH_3 emissions in China estimated based on the results of previous studies are in the range 8.0–18.3 Tg/year (Zhang et al., 2017; Kong et al., 2019), which is indicative of the existence of large uncertainties. Unlike SO_2 and NO_X, which primarily originate from industrial plants, NH_3 mainly originates from agricultural activities, which are more difficult to evaluate. This limits the accuracy of NH_3 and PM concentration estimates simulated using atmospheric chemistry transport models. The main sources of NH_3 emissions in China are fertilizer application and livestock waste; thus, the improvement of NH_3 emission inventories should primarily focus on these two sources (Zhao et al., 2020). To improve NH_3 emission inventory, several environmental factors, including wind speed, temperature, and soil pH, have been considered in some studies (Paulot et al., 2014; Zhang et al., 2018; Zhao et al., 2020). The mass-flow approach, which considers nitrogen transformation at different stages of manure management to improve NH_3 emission inventories from livestock waste, has also been applied (Huang et al., 2012; Zhang et al., 2018).

Monthly variations in NH_3 emissions are primarily caused by fertilizer application based on previous studies (Huang et al., 2012; Zhang et al., 2018). However, fertilizer application-related NH_3 emission inventories need to be further improved for the following reasons. First, in most existing studies, spatial differences in the quantity of fertilizer application in different provinces were considered but spatial variations with respect to the timing of fertilizer application were not, hence the uncertainty in the monthly rate of NH_3 emissions. For example, with respect to winter wheat, in North China, basal dressing is usually conducted from late September to mid-October, while in the Yangtze River Delta region, it is usually conducted from late October to early November. Even in the same province, the difference in fertilizer application dates can be approximately 15 days. In most studies, fertilizer application dates were set to a specific month; however, this is not consistent

https://doi.org/10.5194/acp-2021-439
Preprint. Discussion started: 18 June 2021
© Author(s) 2021. CC BY 4.0 License.
Atmospheric Chemistry and Physics
Discussions

with reality. Farmers in the same province usually apply fertilizers across months, rather than in a specific month. Additionally, the temporal and spatial differences in fertilization dates are critical to the accuracy of the NH_3 emission inventories. Second, there are significant differences in the spatial distribution of planted areas for different crops. This implies that different spatial proxies must be used for different crops. For example, in China, four rice types, namely, early, late, single-season, and middle rice—which cannot be allocated using the same spatial allocation method—are cultivated.

Therefore, in this study, we established a 2016 NH_3 emission inventory with a 5 min × 5 min resolution for mainland China. To improve the accuracy of the emission inventory, we focused on improving the accuracy of NH_3 emissions from fertilizer application, and the latest methods in the literature were used for quantifying emissions from other sources, such as livestock waste. Finally, the inventory accuracy was evaluated using WRF-Chem and available ground station- and satellite-based observation data.

2 Methods and materials

This study was conducted in mainland China. Hong Kong, Macao, and Taiwan were excluded. Fifty emission sources, including fertilizer application, livestock waste, transportation, biomass burning, and agricultural soil, were considered. The categorization of these sources is presented in Table 1. The gridded NH_3 emissions (E_{NH3}) were calculated according to Eq. (1):

$$\boldsymbol{E_{NH_3}} = \sum_i \sum_j \sum_k \boldsymbol{A_{i,j,k}} \times \boldsymbol{EF_{i,j,k}} \tag{1}$$

where *i*, *j*, and *k* represent the specific grid, source type, and month, respectively. *A* represents the activity level (e.g., fertilizer application amounts corresponding to each crop, mileage of motor vehicles, etc.), and *EF* represents the corresponding emission factor.

Reportedly, monthly variations in NH_3 emissions can be primarily attributed to differences in fertilizer application amounts (Huang et al., 2012; Zhang et al., 2018), and fertilizer application-related NH_3 emission inventories have huge uncertainties owing to several factors, including fertilizer type, crop type, fertilization times, fertilization dates, and environmental factors. Therefore, in this study, we focused on improving the accuracy of fertilizer application-related NH_3 emission inventories.

https://doi.org/10.5194/acp-2021-439
Preprint. Discussion started: 18 June 2021
© Author(s) 2021. CC BY 4.0 License.
Atmospheric Chemistry and Physics Discussions

Table 1. NH_3 emission sources in China.

Category	Subcategory	Category	Subcategory
Fertilizer application	urea	Residential & commercial	human excrement
	ammonium bicarbonate (ABC)		indoor firewood combustion
	diammonium phosphate (DAP)		indoor wheat burning
	NPK compound fertilizer (NPK)		indoor rice burning
	other		Indoor maize burning
Livestock waste	beef cattle		domestic coal combustion
	dairy cow		domestic oil combustion
	goat		domestic gas combustion
	sheep	Industry	synthetic ammonia
	rabbit		nitrogen fertilizers production
	horse/donkey/mule		wastewater treatment
	sow		waste landfill
	fattening pig		waste incineration
	camel		coal combustion
	meat duck		oil combustion
	meat goose		gas combustion
	broilers	Other	agricultural soil
	laying hen		nitrogen-fixing plants (soybean)
	laying duck		nitrogen-fixing plants (peanuts)
Traffic	light-duty gasoline vehicles		outdoor straw burning
	heavy-duty gasoline vehicles		Forest fires
	light-duty diesel vehicles		Grassland fires
	heavy-duty diesel vehicles		
	motorcycles		

2.1 Improvement of fertilizer application-related NH_3 emission inventories

Five fertilizer types, including urea, ammonium bicarbonate (ABC), diammonium phosphate (DAP), and complex-fertilizer (NPK), were considered in this study. Additionally, several types of crops that are widely cultivated in China, including early, middle, late, and single-season rice, winter and spring wheat, spring and summer maize, cotton, potato, spring and winter rapeseed, soybean, spring and summer groundnut, sugarcane, sugar beet, tobacco, apple, citruses, pear, and vegetables, were also considered. The respective amounts of the five types of N fertilizers corresponding to the different crop types in each province were calculated as a product of the planted cropland area and the fertilizer application rate per unit area of cropland

https://doi.org/10.5194/acp-2021-439
Preprint. Discussion started: 18 June 2021
© Author(s) 2021. CC BY 4.0 License.

based on data from MARA (2017) and NDRC (2017). Specifically, the following improvements were made to NH_3 emissions inventories from fertilizer application:

(1) In most previous studies, fertilization dates were set such that they did not change in space, but fixed to a specific month; this is not consistent with the actual situation. Therefore, in this study, we comprehensively evaluated the fertilizer application timing and frequency for rice, maize, and wheat crops (these three plants constituted a total of eight sub-categories as shown in Fig. 1) in different regions by collecting data from a large number of studies online (primarily including reports on crop phenology in each province in 2016) and the technical guidelines for field management in each province. The ratio difference between basal dressing and top dressing in the different regions was also considered based on farmer survey data (Wang et al., 2008).

As an example, in 2016, winter wheat in northern Hebei (approximately 1/3 of the wheat-cultivated area in this province) was sown in late September, after which basal fertilizer was applied. This was not the case in the central and southern parts of Hebei, where basal fertilizer was applied in October. Therefore, the dates of basal dressing in Hebei province span two months; 1/3 of the dates were in September, while 2/3 were in October. Similarly, the other two top dressings were applied at the jointing and booting stages, i.e., in late March to early April and late April to early May, respectively. According to the proportion of basal dressing and top dressing on wheat in Hebei, we finally identified the proportion of fertilizer application in each month (basal dressing: 0.2, September; 0.4, October; top dressing: 0.1, March; 0.2, April; and 0.1 in May). Further, the proportion of fertilizer application in each month in Sichuan, which is located in Southwest China, was different from that in Hebei (basal dressing: 0.2, October; 0.4, November; top dressing, 0.1, January; 0.2, February; 0.1 and March). Besides, four sub-categories of rice were considered in this study (early, middle, late, and single-season rice), and given the differences in their fertilization dates in different regions, the fertilization dates varied greatly across the country. Furthermore, a comprehensive assessment of the fertilizer application times and dates corresponding to each crop is of great significance with respect to improving the accuracy of NH_3 emission inventories. Therefore, details regarding the fertilization months and the fertilization ratios corresponding to basal dressing and top dressing for the three main crops were considered (Fig. 1). For other crops, we also identified the corresponding fertilization dates and ratios according to their respective phenological periods by collecting large amounts of data from existing literatures and reports (Zhang et al., 2009; Zhang and Zhang, 2012; Zhang et al., 2018).

https://doi.org/10.5194/acp-2021-439
Preprint. Discussion started: 18 June 2021
© Author(s) 2021. CC BY 4.0 License.
Atmospheric Chemistry and Physics Discussions
Open Access

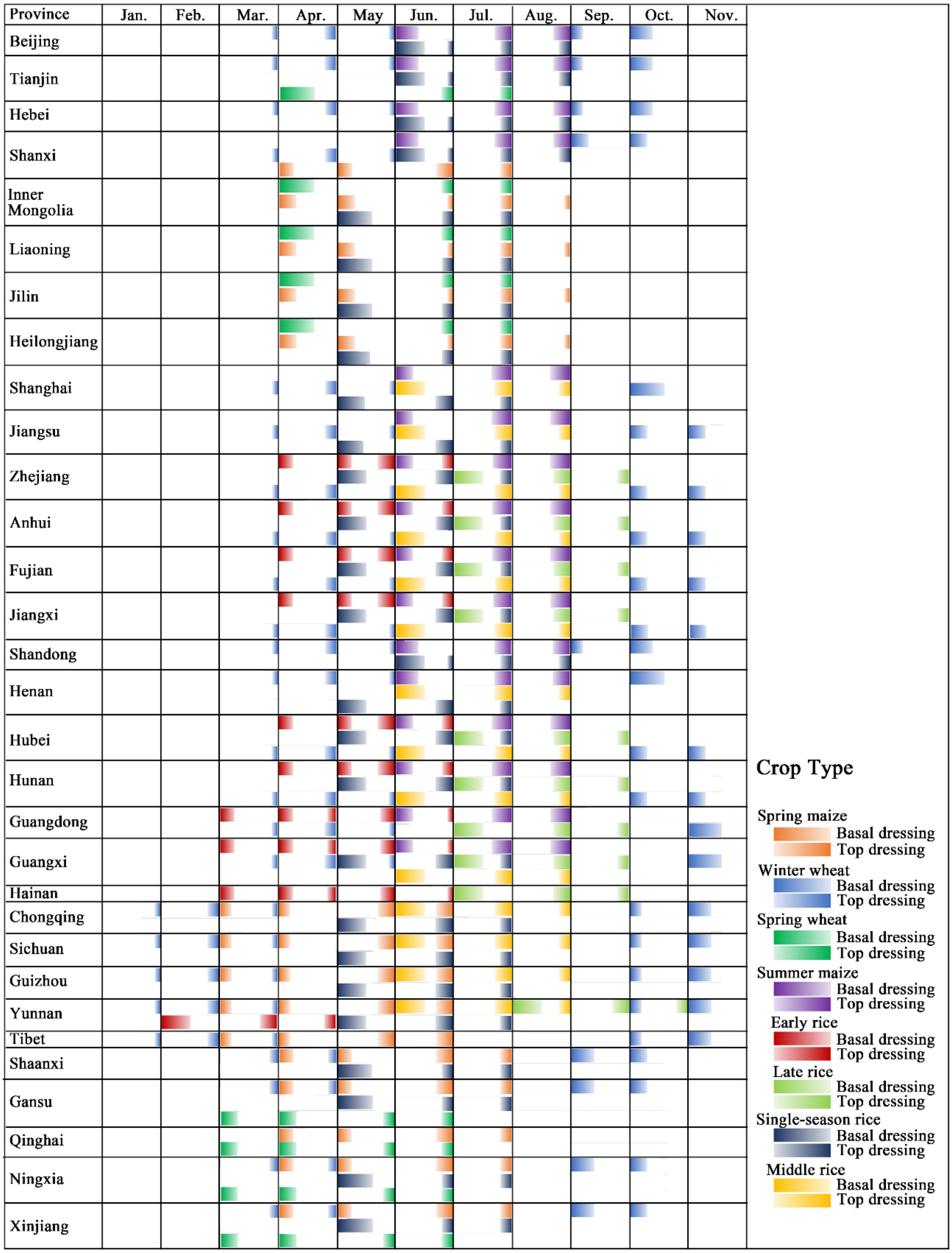

Fig. 1. Basal and topdressing fertilization months and ratios for maize, wheat, and rice in China.

https://doi.org/10.5194/acp-2021-439
Preprint. Discussion started: 18 June 2021
© Author(s) 2021. CC BY 4.0 License.

(2) Given that rice, which is widely cultivated across China, requires nitrogen fertilization, the excessive use of N fertilizer results in sizeable NH_3 emissions (Xia et al., 2020). Fig. 1 shows that compared with other crops, the amount of fertilizer applied to rice in different months is more complex. This implies that more attention should be paid to the spatial allocation of fertilizer quantity corresponding to rice. Therefore, using the spatial distribution of each rice sub-category (i.e., early, late, single-season, and middle rice) as spatial proxies, rather than the overall spatial distribution of rice, can greatly minimize the spatial bias of NH_3 emissions from rice fertilization applications. In this study, we used a variety of data to integrate the spatial distribution of the four rice types in the country. First, spatial distribution data corresponding to the abovementioned rice types in ten provinces of southern China (Henan, Jiangsu, Anhui, Hubei, Hunan, Jiangxi, Zhejiang, Fujian, Guangdong, and Shanghai) were directly obtained from Qiu et al. (2015). This dataset was proposed based on 500 m 8 day composite Moderate Resolution Imaging Spectroradiometer (MODIS) Enhance Vegetation Indices with two bands (EVI2). Its efficiency was validated using data from 763 ground survey sites, and it showed an overall accuracy of 95.02%. Second, for other provinces, we used land use and land cover change (LUCC) data as well as cropping frequency data. Areas where paddy fields overlap with a single cropping frequency were considered as single-season rice areas. Such areas were primarily distributed in Northeast China. Further, areas where paddy fields overlap with a double cropping frequency were considered double-cropping or middle-rice areas. According to the yield of the two rice types in each province, the spatial distribution of early/late rice and middle rice areas can be further distinguished. LUCC data and cropping frequency data with a resolution of 1 km were downloaded from the Resource and Environment Science and Data Center (http://www.resdc.cn/data.aspx?DATAID=184 and http://www.resdc.cn/DOI/doi.aspx?DOIid=42). The spatial distributions of the rice types (single-season rice, middle rice, and early/late rice) are shown in Fig. S1. For other crops, we used the EarthStat dataset on crop harvest area (Monfreda et al., 2008), which provides global crop harvest areas and yields at a 5 min × 5 min resolution.

After completing the above improvements, we further considered the effects of soil properties, agricultural activity, and meteorological conditions (Bouwman et al., 2002; Zhang et al., 2018). The monthly emission factors corresponding to fertilizer application were calculated as follows:

$$EF = EF_0 \times e^{f_{pH} + f_{CEC} + f_{crop} + f_{method}} \times \alpha \qquad (2)$$

where EF_0 represents the baseline emission factors that reported by (Cai et al., 2002; Dong et al., 2009; Zhou et al., 2016) (Table S1), f represents the effects of soil pH, soil cation exchange capacity (CEC), fertilization types (basal dressing and top dressing), and crop types (upland crops and paddy field crops) based on (Bouwman et al., 2002; Zhang et al., 2018). Soil pH and CEC data were obtained from the Harmonized World Soil Database (http://www.fao.org/land-water/databases-and-software/hwsd/en/). Detailed f values are listed in Table S1. Further, α represents the monthly scalar, which was applied to characterize the influence of meteorological factors on NH_3 emissions (Gyldenkaerne et al., 2005; Zhang et al., 2018).

https://doi.org/10.5194/acp-2021-439
Preprint. Discussion started: 18 June 2021
© Author(s) 2021. CC BY 4.0 License.

$$\alpha = (e^{0.0223T_i + 0.0419W_i}) / (\frac{1}{12}\sum_{i=1}^{12} e^{0.0223T_i + 0.0419W_i}) \quad (3)$$

where T_i and W_i represent 2 m air temperature (°C) and 10 m wind speed (m/s) for a given month, i, respectively. T and W were processed using ECMWF ERA5 Reanalysis data (https://www.ecmwf.int/en/forecasts/datasets/reanalysis-datasets/era5).

2.2 NH_3 emission from livestock waste

Traditional NH_3 emissions from livestock waste are usually calculated as a product of livestock population and the corresponding emission factors. In this study, a more process-based mass-flow approach was applied, considering nitrogen transformation at the different stages of manure management (Huang et al., 2012; Kang et al., 2016; EEA, 2019). The total ammoniacal nitrogen (TAN) amount was obtained using the annual livestock amount, the daily amount, and the nitrogen content of urine and feces for each livestock category. Details in this regard are provided in Table S2. The outdoor and indoor generated TAN contents were separately estimated based on the proportion of the time each livestock category spent indoor and outdoor, respectively. There are three main livestock breeding systems in China, namely grazing, free-ranging, and intensive livestock breeding systems. Among them, half of the livestock urine and feces corresponding to the grazing and free-range systems are discharged indoors. However, for intensive livestock breeding, all the livestock urine and feces are discharged indoors (MEP, 2014). Grazing is practiced only in pastoral and semi-pastoral areas, i.e., in 13 provinces (Hebei, Shanxi, Inner Mongolia, Liaoning, Jilin, Heilongjiang, Sichuan, Yunnan, Tibet, Gansu, Qinghai, Ningxia, and Xinjiang). According to the nitrogen flow and phase of manure management, the activity levels were classified under seven categories: outdoor, housing solid, housing liquid, storage solid, storage liquid, spreading solid, and spreading liquid. Thus, NH_3 emissions from livestock were calculated as a product of the TAN of the seven categories and the corresponding emission factors (Huang et al., 2012; MEP, 2014; Kang et al., 2016). Livestock production in each province was obtained from MARA (2017) and NBS (2017c).

After estimating the NH_3 emissions corresponding to the three livestock breeding systems in different provinces, we allocated the grazing emissions to grids based on grassland areas in the pastoral and semi-pastoral areas and allocated the emissions from free-range and intensive livestock production based on the corresponding rural residential areas. In addition to emissions from fertilizer applications, the influence of meteorological factors on NH_3 emissions from livestock waste was also considered. For outdoor NH_3 emissions, we considered the influence of monthly temperature and wind speed using Eq. (3), while accounting only for air temperature for indoor emissions (Zhang et al., 2018).

2.3 NH_3 emission from other sources

NH_3 emissions from combusted crop residue were estimated based on crop yield, grain-to-straw ratio, combustion ratio, and combustion efficiency (Zhou et al., 2017). The contribution of firewood combustion to NH_3 emissions was derived from (Cong et al., 2017). Additionally, grassfire and forest fire data were obtained by coupling MCD14ML and MCD64A1 fire products based on previous studies (Qiu et al., 2016; Li et al., 2018). The emissions originating from human excrement were calculated based on the daily excretion data corresponding to children and adults, rural populations, and the fraction of tatty latrines in each province (Huang et al., 2012). The emissions corresponding to the total mileage for each vehicle category were calculated using the number of vehicles and the average annual mileage. Further, NH_3 emissions from other sources were determined following the approaches proposed by previous studies (Huang et al., 2012; Kang et al., 2016). Relevant data were obtained from NBS, 2017c, a, b, and d. The specific emission factors and spatial allocation methods for each source are listed in Table S3.

2.4 NH_3 emission inventory uncertainty and accuracy evaluation

The uncertainty of NH_3 emissions was calculated using the Monte Carlo method, which has been widely used in various inventory studies (Zhao et al., 2011; Kang et al., 2016; Li et al., 2019a). Based on previous studies, we assumed that the uncertainties in the activity levels and emission factors were uniformly and normally distributed. The detailed parameters of the CVs of the two datasets were derived from Huang et al. (2012). The NH_3 emission calculations were replicated 10,000 times with a random selection of all the inputs.

Further, the inventory established in this study and the MEIC inventory were applied to WRF-Chem to evaluate the inventory accuracy. The simulations were conducted for January and July 2016 given that these two months are associated with the least and largest NH_3 emission amounts, respectively. The simulation domain with a resolution of 27 km is shown in Fig. 2, which covers most parts of North, East, Central, and South China. Areas with high NH_3 emission density in China are shown in Fig. 4. Inventory accuracy was further assessed using WRF-Chem and available ground station- and satellite-based observations. First, we compared the NH_3 VCDs obtained using infrared atmospheric sounding interferometer (IASI) satellite observations and with those from WRF-Chem using our estimated inventory and MEIC. Daily IASI NH_3 VCDs were downloaded from the ESPRI data center (https://cds-espri.ipsl.upmc.fr/etherTypo/index.php?id=1700&L=1). The mean local solar overpass times were 9:30 am and 9:30 pm at the equator. Further, in this study, only the IASI NH_3 VCDs collected from the morning orbit, which are generally more sensitive to NH_3 emissions owing to their higher thermal contrast, were considered (Van Damme et al., 2014; Van Damme et al., 2015). Furthermore, to ensure comparison accuracy, the average simulated NH_3 concentrations at 09:00 and 10:00 local time were applied to calculate the simulated NH_3 VCDs (Zhao et al., 2020). Second, based on ground observation data, we compared the simulated NH_3 concentrations using WRF-Chem. Specifically, 2016 observed NH_3 concentrations were obtained from the Ammonia Monitoring Network in China (AMoN-China) (Pan et al., 2018), and the simulation domain of WRF-Chem consisted of 30 samples from AMoN-China (Fig. 2).

https://doi.org/10.5194/acp-2021-439
Preprint. Discussion started: 18 June 2021
© Author(s) 2021. CC BY 4.0 License.

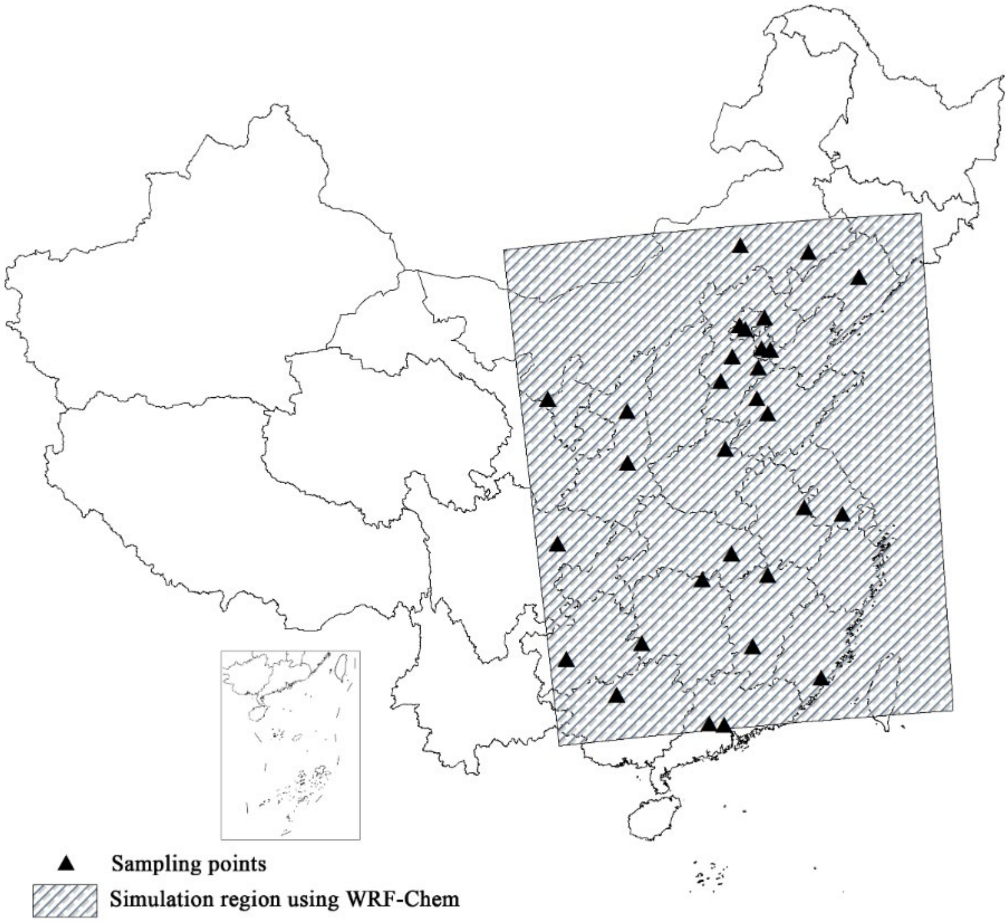

Fig. 2. WRF-Chem simulation domain and sampling points (Ammonia Monitoring Network, China).

3 Results and discussion

3.1 NH_3 emissions and main sources in China

In 2016, the total atmospheric ammonia emission in mainland China was 12.11 Tg (9.29−15.54 Gg, 95% confidence interval based on a Monte Carlo simulation), and the emission density was 1.28 t/km^2. This total NH_3 emission amount was found to be approximately three-fold that obtained for Europe (4.18 Tg) (Backes et al., 2016), and represented approximately 38 and 27% of Asian and global NH_3 emissions, respectively (Bouwman et al., 1997; Kurokawa and Ohara, 2020). Further, this estimated emission was relatively close to the improved emissions based on AMoN-China and the Ensemble Kalman Filter (13.1 Tg). It was also close to the improved bottom-up emission (11.7 Tg) reported by (Zhang et al., 2018). However, it was approximately 25% higher than that reported by (Kang et al., 2016), and approximately 15% lower than the REAS emission

https://doi.org/10.5194/acp-2021-439
Preprint. Discussion started: 18 June 2021
© Author(s) 2021. CC BY 4.0 License.

(Kurokawa and Ohara, 2020). Table 2 presents a quantitative comparison of this emission inventory with those reported in previous studies.

Table 2. Comparison of NH_3 emissions with those obtained in other Studies.

Source	Base year	Total	References
EDGARv5.0	2015	8.9	https://edgar.jrc.ec.europa.eu/dataset_ap50
REASv3	2015	14.1	(Kurokawa and Ohara, 2020)
MEIC	2016	10.3	http://meicmodel.org/
MASAGE_NH3	2007	8.4	(Paulot et al., 2014)
Zhang et al.	2015	15.6	(Zhang et al., 2017)
Huang et al.	2006	9.8	(Huang et al., 2012)
Xu et al.	2008	8.4	(Xu et al., 2016)
Xu et al.	2010	10.7	(Xu et al., 2015)
Kang et al.	2012	9.7	(Kang et al., 2016)
Kong et al.	2016	13.1	(Kong et al., 2019)
Zhang et al.	2008	11.7	(Zhang et al., 2018)
Streets et al.	2000	13.6	(Streets et al., 2003)
Zhao et al.	2010	9.8	(Zhao et al., 2013)

Similar to other studies, livestock waste (5.42 g) and fertilizer application (4.67 g) were identified as the two largest NH_3 emission sources in China, with their contribution to the total NH_3 emission amount reaching over 80% (Fig. 3). Other sources included synthetic ammonia (0.43 Tg), agriculture soil (0.29 Tg), indoor biomass combustion (0.30 Tg), domestic coal combustion (0.26 Tg), nitrogen fertilizer production (0.22 Tg), transportation (0.10 Tg), and others (0.4 Tg), with contributions to the total emission amount as follows: 3.5, 2.4, 2.5, 2.2, 1.8, 0.9, and 3.3%, respectively.

Similar to previously reported results, with respect to the different fertilizers considered, urea was identified as the major contributor to NH_3 emissions, accounting for approximately 45.4% of fertilizer type-related NH_3 emissions (Fig. 3). Kang et al. (2016) observed that ABC is an important source of fertilizer type-related NH_3 emission source owing to its high volatility; however, in 2016, it only accounted for 12.9% of fertilizer type-related NH_3 emissions. This is because, in recent years, there has been a significant decrease in the proportion of ABC-related emissions in China owing to the decrease in the amounts of ABC applied to the three main crops, maize, rice, and wheat (from 26.55 kg/hm^2 in 2011 to 10.80 kg/hm^2 in 2016, i.e., a 59.32% reduction). However, emissions related to complex fertilizers have increased by 33.61% (NDRC, 2017). Specifically, NPK fertilizers have become the second-largest source of fertilizer type-related NH_3 emissions in China (26.7%). Therefore, replacing complex fertilizers with ABC might reduce fertilizer type-related NH_3 emissions to a certain extent.

https://doi.org/10.5194/acp-2021-439
Preprint. Discussion started: 18 June 2021
© Author(s) 2021. CC BY 4.0 License.

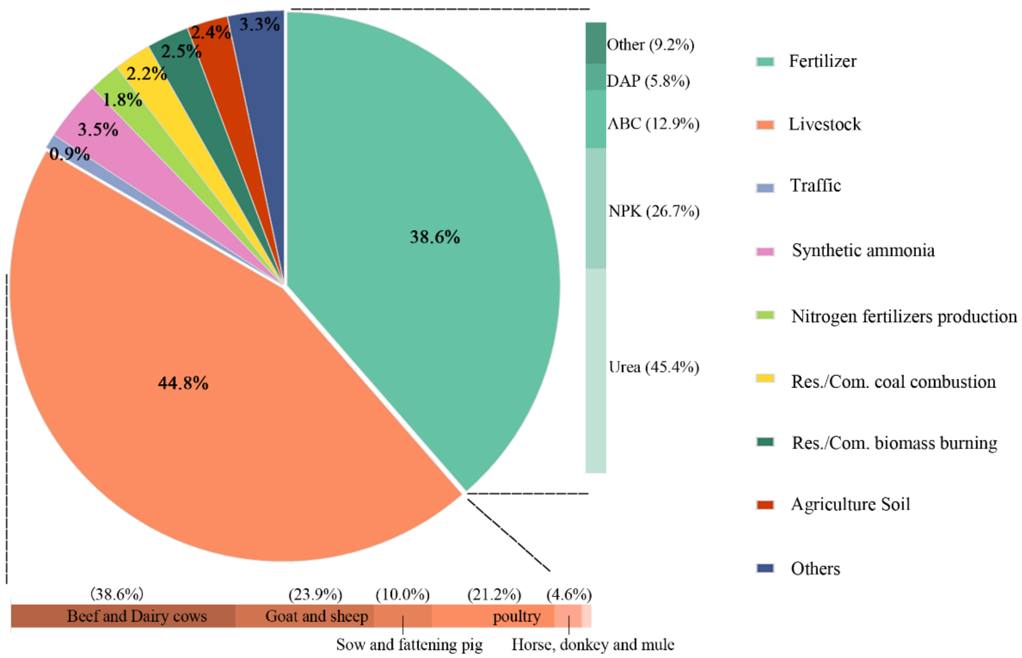

Fig. 3. Contributions of different sources (%) to NH_3 emissions in mainland China (2016).

Maize fertilization contributed the most to NH_3 emissions (1.21 Tg), accounting for 25.94% of fertilizer application-related emissions. This observation could be primarily attributed to the planting area of maize—the largest of the total crop area, up to 22.06% (Nbs, 2017a). Moreover, the maize fertilization dates were concentrated in summer, and the high temperature further increased the NH_3 emission rate. It is also worth noting that vegetable fertilization has become the second-largest fertilizer application-related NH_3 emission source (0.89 Tg), i.e., 19.06%, based on our estimation. In addition to the relatively large area corresponding to vegetable cultivation in China, vegetable-related fertilizer application rates were higher than those corresponding to the three major crops considered in this study (Wang et al., 2018). The amounts of urea, DAP, and NPK used in the fertilization of vegetable-cultivated land were 1.29, 1.77, and 1.40 times those applied in cropland for cultivating the three main crops, respectively. This is due to the lack of scientific fertilization methods for vegetables in China (Ndrc, 2017). Further, rice and wheat fertilization accounted for 17.47 and 14.80% of fertilizer application-related emissions, respectively. Furthermore, NH_3 emissions corresponding to the above four crop types accounted for more than 75% of the total NH_3 emissions from fertilizer application.

Regarding livestock waste, beef and dairy cow waste were the largest contributors (38.6%) to livestock waste-related NH_3 emissions. This was followed by goats and sheep waste (23.9%) and poultry waste (21.2%); this is consistent with (Kang et al., 2016). Further, we analyzed animal breeding system-related nitrogen transformation and migration and observed that

https://doi.org/10.5194/acp-2021-439
Preprint. Discussion started: 18 June 2021
© Author(s) 2021. CC BY 4.0 License.

the contributions of the four manure management stages to NH_3 emissions were 1.06, 1.14, 0.85, and 2.73 Tg for outdoor (19.60%), housing (21.10%), manure storage (15.65%) and manure spreading (43.65%), respectively. This is also consistent with the results of Xu et al. (2017). Our analysis also showed that the free-range system is the largest contributor to livestock waste-related NH_3 emissions, i.e., 2.80 Tg, which accounted for 51.6% of the total livestock waste-related emissions. This was followed by the intensive system (1.92 Tg, 35.47%), and lastly, the grazing system (0.70 Tg, 12.90%). The rapid increase in the proportion of intensive livestock raising has slowed down NH_3 emissions to a certain extent (Qian et al., 2018).

3.2 Geographical distribution of NH_3 emissions

The spatial distribution of NH_3 emissions in 2016 is shown in Fig. 4, from which a strong spatial variability is evident. The highest NH_3 emission density, 6.96 t/km^2, which was 5.44-fold higher than the national average (1.28 t/km^2) was observed in Shandong. Further, the number of provinces with NH_3 emissions above this average national density value was 21, and the provinces with emission densities exceeding 3 t/km^2 included: Shandong (6.96 t/km^2), Henan (6.81 t/km^2), Jiangsu (5.01 t/km^2), Tianjin (4.43 t/km^2), Hebei (4.39 t/km^2), and Anhui (3.41 t/km^2). Although these six provinces account for only 8.08% of China's land area, their contribution to NH_3 emissions in China was 33.74%. These provinces are all concentrated in North China, hence its high NH_3 emission density.

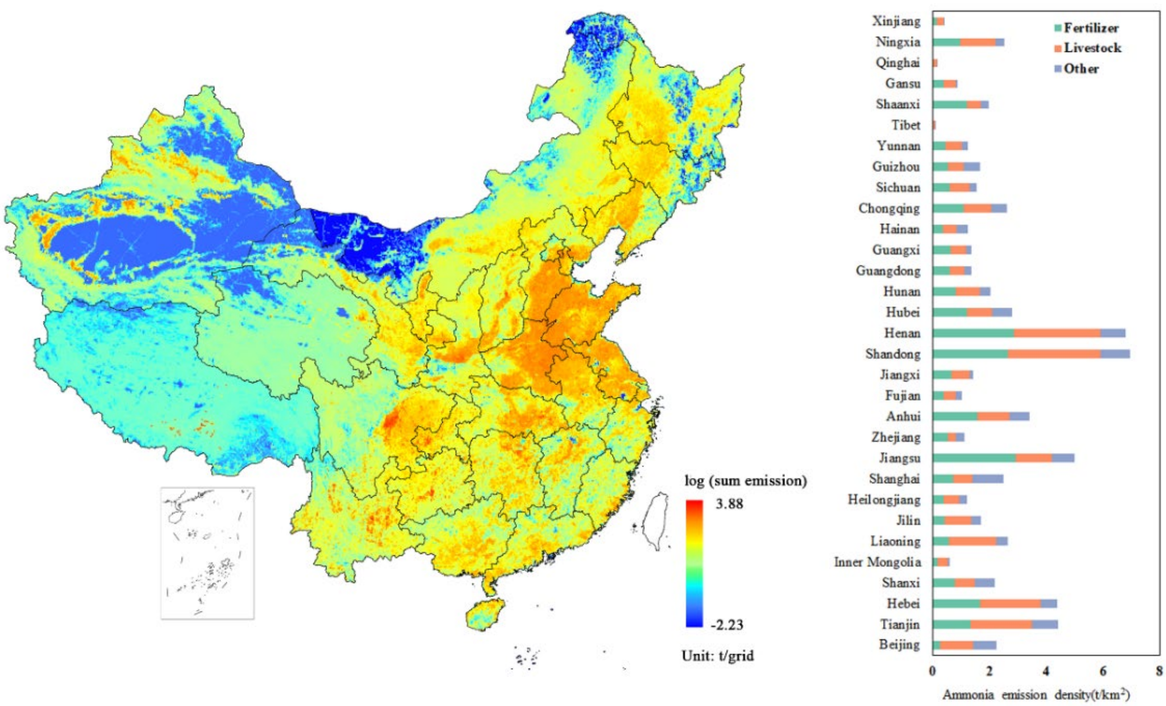

Fig. 4. Geographical distribution of 2016 NH_3 emissions and emission densities in China.

https://doi.org/10.5194/acp-2021-439
Preprint. Discussion started: 18 June 2021
© Author(s) 2021. CC BY 4.0 License.

Shandong and Henan provinces not only had the two top emission densities, their emissions were also the top two in mainland China, reaching 1.13 and 1.08 Tg, respectively. These high emissions could be primarily attributed to the following reasons: First Shandong and Henan are the major agricultural provinces in China. Although they represent only 3.40% of the total land area of mainland China, in 2016, they accounted for 38.43, 17.74, and 16.31% of wheat, maize, and vegetables yields, respectively (NBS, 2017a). The NH_3 emissions corresponding to these three crops were remarkable, accounting for 80.35 and 79.23% of the fertilizer application-related NH_3 emissions in Shandong and Henan, respectively. Second, there are a large number of livestock farms in these two provinces (Hu et al., 2017). Specifically, beef cattle and poultry breeding in the two provinces also resulted in high NH_3 emissions from livestock waste, and only these two provinces showed livestock waste-related emission densities above 3 t/km^2.

Furthermore, Jiangsu province had the highest fertilizer application-related emission density (2.94 t/km^2) in China, which was 5.96 times above the national average. This is not only due to the relatively large crop area in this province, but also, more importantly, the fertilizer application rates in this province were much higher than in other provinces. For example, the rates of urea application to wheat and rice, which together constitute the largest planting area in Jiangsu Province, were 191.40 and 223.80 kg/hm^2, respectively, i.e., 1.42- and 1.97-fold higher than the national average value, respectively. Further, emissions from fertilizer application accounted for 58.68% of the total NH_3 emissions in Jiangsu. Therefore, enhancing nitrogen fertilizer use efficiency is an important and effective strategy by which NH_3 emissions in Jiangsu can be controlled.

The NH_3 emissions in Sichuan and Xinjiang in Western China were also high, ranking fourth (0.75 Tg) and sixth (0.68 Tg) in the country, respectively. Specifically, in Sichuan, rice and vegetable cultivation was identified as the principal fertilizer application-related NH_3 emission sources, (25.73 and 20.85%, respectively), while cotton cultivation was identified as the main emission source in Xinjiang (49.20%). These results reflect the huge differences in planting structure in China. In terms of livestock breeding, the largest emission sources in Sichuan were beef cattle and dairy cow breeding (25.43%) and goat and sheep breeding (23.79%), while the total contribution of these two livestock breeding practices in Xinjiang was 86.57%, indicating significant differences in dietary habits in the different provinces China. These findings also indicate that different livestock waste-related NH_3 emission reduction strategies are needed for different regions. The specific NH_3 emissions corresponding to different emission sources in the different provinces are shown in Table 3, and the spatial distribution of NH_3 emissions from fertilizer application, livestock waste, and other sources are shown in Fig. 4.

https://doi.org/10.5194/acp-2021-439
Preprint. Discussion started: 18 June 2021
© Author(s) 2021. CC BY 4.0 License.
Atmospheric Chemistry and Physics Discussions
Open Access
EGU

310 **Table 3. NH_3 emissions (Gg) from various sources in the different provinces in mainland China.**

Province	Fertilizer					Livestock			Other
	Urea	ABC	DAP	NPK	Other	Free	Grazing	Intensive	
Beijing	2.08	0.05	0.36	1.79	0.24	4.10	0.00	15.02	13.53
Tianjin	8.48	0.62	1.94	4.10	0.78	7.75	0.00	17.98	11.14
Hebei	144.97	17.68	28.20	107.11	15.08	185.17	20.51	199.82	107.78
Shanxi	58.93	8.96	10.48	15.15	28.56	48.43	1.41	60.05	112.35
Inner Mongolia	108.06	34.72	30.99	9.97	8.74	40.72	242.87	148.32	79.26
Liaoning	34.11	1.64	6.89	28.43	13.93	118.52	21.97	106.43	56.99
Jilin	37.45	0.85	7.76	17.86	19.93	86.25	25.61	64.39	63.50
Heilongjiang	102.53	0.00	25.23	37.76	18.22	94.23	46.40	105.97	123.07
Shanghai	3.76	0.28	0.02	1.75	0.17	1.92	0.00	3.47	8.90
Jiangsu	178.11	15.06	2.83	86.35	19.56	50.58	0.00	80.92	81.08
Zhejiang	27.87	4.50	0.04	17.26	6.86	16.90	0.00	12.97	32.35
Anhui	107.86	5.00	1.04	82.95	24.12	106.16	0.00	52.50	98.85
Fujian	9.34	17.95	0.01	12.18	7.00	24.37	0.00	28.25	27.29
Jiangxi	44.85	4.27	0.04	46.38	14.21	80.49	0.00	27.27	23.39
Shandong	130.75	24.10	20.42	196.05	40.66	258.12	0.00	252.73	162.09
Henan	165.76	59.08	9.18	174.22	65.62	340.50	0.00	164.65	148.63
Hubei	52.13	78.79	0.63	65.15	29.63	92.95	0.00	72.38	128.85
Hunan	61.72	36.60	0.31	44.12	31.02	137.98	0.00	40.30	81.46
Guangdong	46.33	9.94	0.08	50.38	2.04	66.26	0.00	24.40	43.17
Guangxi	65.03	9.89	0.40	59.97	17.49	111.96	0.00	18.50	42.76
Hainan	4.50	0.09	0.00	6.39	1.29	14.91	0.00	2.08	13.99
Chongqing	27.76	24.63	0.05	31.70	6.19	68.94	0.00	10.62	45.50
Sichuan	103.66	106.80	0.18	60.43	23.38	231.96	44.73	62.37	119.67
Guizhou	57.67	4.47	0.31	18.49	13.43	82.93	0.00	17.67	102.41
Yunnan	109.41	23.92	1.29	24.32	12.81	189.80	1.63	35.94	78.72
Tibet	0.50	0.38	0.01	0.15	0.09	54.33	52.32	5.84	6.94
Shaanxi	110.84	85.87	21.93	27.75	1.55	77.98	0.00	24.59	59.27
Gansu	112.96	5.27	27.01	13.36	6.88	70.96	50.25	62.81	32.24
Qinghai	5.79	0.52	2.21	0.41	0.17	3.76	69.85	19.27	25.99
Ningxia	18.76	19.07	7.85	4.93	0.00	15.96	18.16	30.46	15.56
Xinjiang	177.39	1.10	62.57	2.61	1.48	114.87	103.78	155.04	64.84
Sum	2119.36	602.09	270.23	1249.44	431.14	2799.77	699.49	1923.02	2011.59

https://doi.org/10.5194/acp-2021-439
Preprint. Discussion started: 18 June 2021
© Author(s) 2021. CC BY 4.0 License.

3.3 Monthly variation of NH_3 emissions

The monthly variation of NH_3 emissions from the main emission sources is shown in Fig. 5. Unlike the monthly emission trends of pollutants, such as $PM_{2.5}$ and NO_x, NH_3 emissions presented a high trend in summer and a low one in winter. The highest and lowest emissions (1.68 and 0.55 Tg, respectively) were recorded in July and January, respectively; the July to January emission ratio was 3.08, which is close to the ratio obtained based on IASI satellite observations (2.85), and larger than that based on MEIC data (1.72).

Further, a comparison of the monthly trend of NH_3 emissions based on IASI satellite observations with that obtained in this study showed a strong correlation between the two trends ($R^2 = 0.85$). Owing to temperature changes, livestock waste-related emissions increased slowly from 0.30 Tg in January to 0.60 Tg in July, and then gradually decreased to 0.34 Tg in December. Additionally, the monthly fluctuation of fertilizer application-related NH_3 emissions was greater than that of livestock waste-related emissions (Fig. 5(a)). Fertilizer application-related NH_3 emissions in July were 11.79 times than those observed in January. These monthly variations in NH_3 emission amounts could be primarily attributed to the effect of the farming season on fertilization. Thus, we further analyzed monthly NH_3 emission variation with respect to different crops (Fig. 5(b)). The results obtained it was observed that maize and rice fertilization in summer was primarily responsible for the increase in NH_3 emissions in China. For example, NH_3 emissions from maize and rice fertilization in July accounted for 44.89 and 27.61% of the total fertilizer application-related NH_3 emissions, followed by cotton fertilization (8.59%). Even though wheat also contributed significantly to NH_3 emissions (14.80%), the emissions were primarily concentrated in April and September, accounting for 36.38 and 23.47% of the emissions from fertilizer application in these months, respectively.

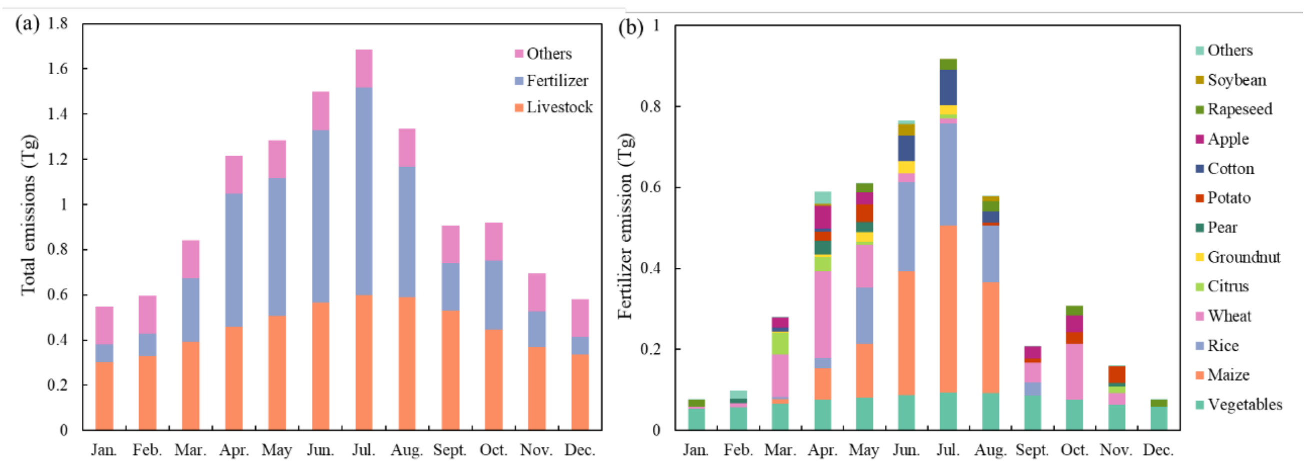

Fig. 5. Monthly NH_3 emissions from: (a) Different sources and (b) Different crops.

https://doi.org/10.5194/acp-2021-439
Preprint. Discussion started: 18 June 2021
© Author(s) 2021. CC BY 4.0 License.

3.4 Verification of the accuracy of the NH_3 emission inventory

3.4.1 Temporal accuracy of NH_3 emission inventory

We verified the accuracy of the monthly NH_3 emission trends obtained in this study as well as that based on MEIC via comparison with IASI satellite observations. Thus, it was observed that the monthly trend of our inventory was significantly more correlated with the IASI data ($R^2 = 0.85$) than the MEIC inventory ($R^2 = 0.70$). The correlations of the monthly trends of the IASI data and the two inventories were also compared for different regions in China. The results showed that except for Central China, the correlations of the monthly trends between our inventory and IASI data were higher than those between the MEIC inventory and IASI data (Table 4). Additionally, the July to January emission ratio was used to further verify inventory accuracy, and it was observed that our emission inventory ratios were close to those based on IASI data for all regions of China. However, the ratios based on MEIC data were relatively lower, possibly owing to the underestimation of NH_3 emissions in summer.

Table 4. Comparison of the monthly NH_3 emission trends corresponding to IASI satellite observations with the two inventories.

Region	R^2		July/Jan ratio		
	IASI vs. OUR	IASI vs. MEIC	IASI	OUR	MEIC
Northeast China	**0.92**	0.67	3.81	3.94	1.66
Northern China	**0.79**	0.69	2.77	3.51	1.66
Eastern China	**0.62**	0.53	4.63	3.51	1.81
Southern China	**0.58**	0.33	3.93	2.01	1.84
Central China	0.47	0.57	4.09	2.83	1.75
Southwest China	**0.43**	0.31	2.22	2.02	1.61
Northwest China	**0.79**	0.59	2.16	3.58	1.77
Beijing-Tianjin-Hebei region	**0.59**	0.58	3.95	3.35	1.69
Yangtze River Delta region	**0.62**	0.49	5.45	3.98	1.95
Mainland China	**0.84**	0.70	2.85	3.08	1.72

3.4.2 Spatial accuracy of our NH_3 emission inventory

We compared the simulated NH_3 concentration using WRF-Chem and ground observations obtained from AMoN-China (Fig. 6(a)). Thus, it was observed that the spatial accuracy of our inventory was better than that of the MEIC inventory. Additionally, the simulated NH_3 concentration based on our inventory showed high correlation with ground-based observations ($R^2 = 0.55$), with a slope of 0.9 (approximately equal to 1). However, the correlation between the simulated concentration based on MEIC data and ground-based observations was relatively low, $R^2 = 0.21$, with a slope of 0.32 (Fig. 6(b)). These findings indicate that the MEIC inventory possibly underestimates NH_3 emissions.

https://doi.org/10.5194/acp-2021-439
Preprint. Discussion started: 18 June 2021
© Author(s) 2021. CC BY 4.0 License.

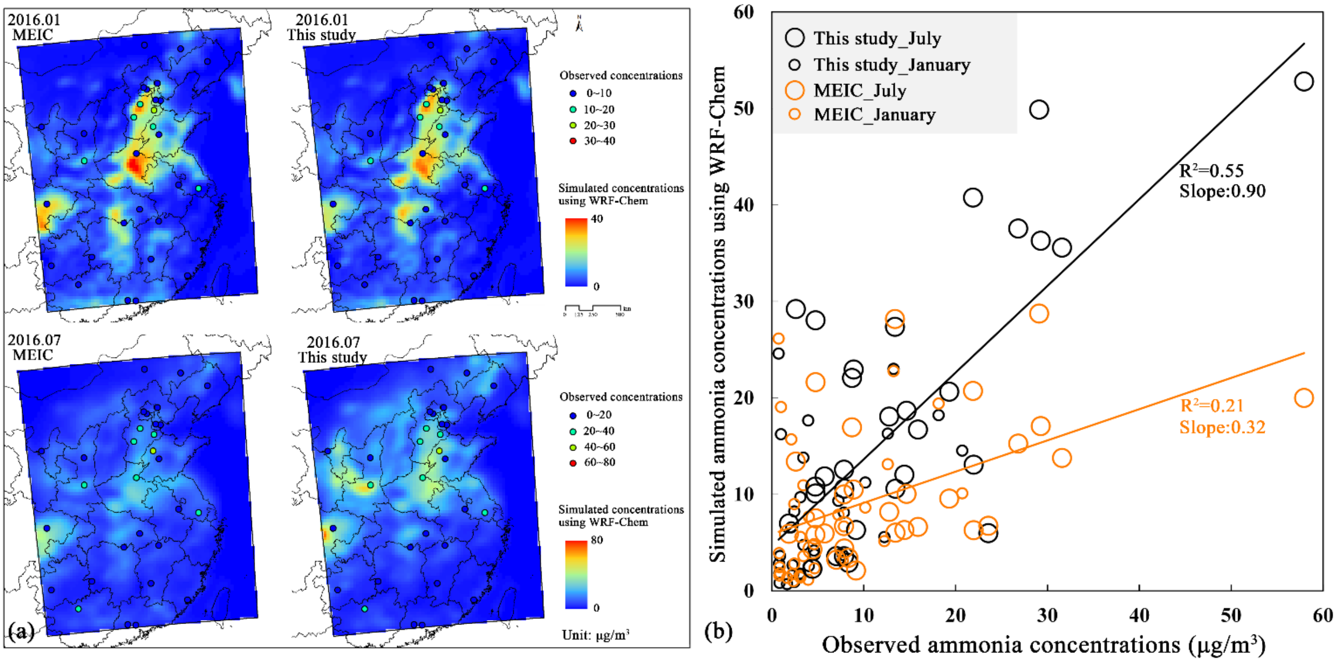

Fig. 6. (a) Comparison of the spatial accuracies of different inventories. (b) Comparison of observed and simulated NH_3 concentrations in January and July (Circles of different sizes represents different months).

We also compared the NH_3 VCDs based on IASI satellite observations with those from WRF-Chem based on the inventory established in this study and that based on MEIC data at a 0.25 resolution (Fig. 7). The distribution of NH_3 VCDs simulated using the two inventories is shown in Fig. S2. In general, the spatial accuracy of our inventory was better than that of the MEIC inventory, and in July, the coefficient of determination obtained by fitting the simulated NH_3 VCDs using our inventory and IASI-based VCDs was 0.42, significantly higher than that fitted using the NH_3 VCDs based on MEIC data and IASI data (0.28). Similar to the results obtained after comparison with AMoN-China data, we observed that the MEIC-based NH_3 emissions were significantly underestimated for July (a slope of only 0.22). The normalized mean biases (NMBs) and normalized mean errors (NMEs) between IASI VCDs and our simulated NH_3 VCDs were 6 and 47%, respectively. For MEIC simulated NH_3 VCDs, they were 42.46 and 56.17%, respectively. Further, in January, the spatial accuracy of our inventory (NMB, -23.76%; NME, 67.06%) was slightly better than that corresponding to MEIC (NMB, -26.47%; NME, 69.84%). However, we found that the correlations between the NH_3 VCDs simulated using the two inventories and IASI VCDs were low, primarily owing to the uncertainty of the IASI VCDs and numerous invalid values for January (Van Damme et al., 2017; Chen et al., 2020).

https://doi.org/10.5194/acp-2021-439
Preprint. Discussion started: 18 June 2021
© Author(s) 2021. CC BY 4.0 License.
Atmospheric Chemistry and Physics Discussions

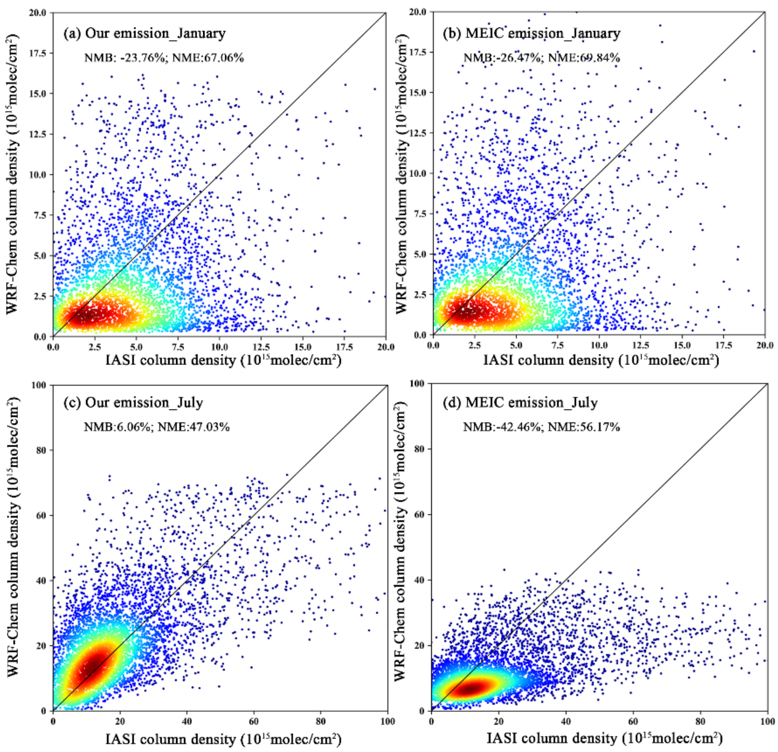

Fig. 7. Comparison between IASI-based VCDs and simulated NH_3 VCDs corresponding to: (a) Our emission, January, (b) MEIC emission, January, (c) Our emission, July, and (d) MEIC emission, July.

4 Conclusion

NH_3—an important component of the nitrogen cycle—can accelerate the formation of SIAs. Even though several effective measures have been taken to reduce SO_2 and NO_X emissions, the concentration of NH_3 in the atmosphere continues to rise, and unfortunately, gridded NH_3 emissions inventories for China still have large uncertainties. Therefore, establishing and improving such gridded NH_3 emission inventories can optimize the simulation results of chemical transport models such as WRF-Chem; this is of great significance in regional pollution control. Therefore, in this study, we focused on improving NH_3 emission inventories owing to fertilizer application. To this end, we comprehensively evaluated the times and dates of fertilizer application to the major crops that are cultivated in different regions in China, improved the spatial allocation methods for NH_3 emissions from different rice types, and established a gridded NH_3 emission inventory for mainland China (2016) with a 5 min × 5 min resolution.

The atmospheric ammonia emission in mainland China was found to be 12.11 Tg, and the average emission density was 1.28 t/km^2. Livestock waste (44.8%) and fertilization application (38.6%) were identified as the two major NH_3 emission

© Author(s) 2021. CC BY 4.0 License.

sources in China. On the one hand, beef and dairy cow breeding contributed the most to livestock waste-related NH_3 emissions, with the free-range system accounting for more than half of the emissions from livestock waste. On the other hand, urea (45.4%) and NPK (26.7%) applications were identified as the main fertilizer application-related NH_3 emission sources. NH_3 emissions from the cultivation of maize, vegetables, rice, and wheat (25.94, 19.06, 17.47, and 14.8%, respectively) accounted for over 75% of the total emissions from fertilizer application, and in addition to showing the top two emission densities, Shandong and Henan Provinces also showed the top two emissions amounts in mainland China, reaching 1.13 and 1.08 Tg, respectively. The highest emission (1.68 Tg) was recorded in July and the lowest (0.55 Tg) in January. We also observed a strong correlation between the monthly trend of NH_3 emissions based on IASI satellite observations and that established in this study ($R^2 = 0.85$). This monthly variation in NH_3 emissions was primarily due to the effect of the farming season on fertilization process. Specifically, the fertilization of maize and rice in summer was primarily responsible for the increase in NH_3 emissions in China. Additionally, the evaluation of the spatial and temporal accuracies of the NH_3 emission inventories obtained in this study using WRF-Chem and AMoN-China observations as well as IASI VCDs indicated that the accuracy of our inventory is better than that of other inventories.

Data availability. All data used in this paper are available upon request from the corresponding author Hong Liao (hongliao@ nuist.edu.cn).

Author contributions. Baojie Li and Hong Liao designed and performed this study. Lei Chen performed the WRF-Chem simulations and data analysis. Jianbing Jin contributed the monthly IASI data. Weishou Shen, Teng Wang, Pinya Wang and Yang Yang discussed the results and commented on the paper.

Competing interests. The authors declare that they have no conflict of interest.

Acknowledgements. We acknowledge the Centre National d'Études spatiales (CNES, France), and MEIC team for making their data publicly available. We also thank Yuepeng Pan from Institute of Atmospheric Physics, Chinese Academy of Sciences, for publishing the observed NH_3 concentrations data (AMoN-China) (Pan et al., 2018), which is helpful for the verification of the NH_3 emission inventory.

Financial support. This research has been supported by the National Natural Science Foundation of China [grant 42007381], the Natural Science Foundation of Jiangsu Province [grant BK20200812], and the National Key Research and Development Program of China [grant 2020YFA0607803].

https://doi.org/10.5194/acp-2021-439
Preprint. Discussion started: 18 June 2021
© Author(s) 2021. CC BY 4.0 License.

Atmospheric Chemistry and Physics Discussions

References

Backes, A., Aulinger, A., Bieser, J., Matthias, V., and Quante, M.: Ammonia emissions in Europe, part I: Development of a dynamical ammonia emission inventory, Atmos Environ, 131, 55-66, 10.1016/j.atmosenv.2016.01.041, 2016.

Bouwman, A., Boumans, L., and Batjes, N.: Estimation of global NH3 volatilization loss from synthetic fertilizers and animal manure applied to arable lands and grasslands, Global Biogeochemical Cycles, 16, 8-1-8-14, 2002.

Bouwman, A. F., Lee, D. S., Asman, W. A. H., Dentener, F. J., Van Der Hoek, K. W., and Olivier, J. G. J.: A global high-resolution emission inventory for ammonia, 11, 561-587, https://doi.org/10.1029/97GB02266, 1997.

Cai, G. X., Chen, D. L., Ding, H., Pacholski, A., Fan, X. H., and Zhu, Z. L.: Nitrogen losses from fertilizers applied to maize, wheat and rice in the North China Plain, Nutrient Cycling in Agroecosystems, 63, 187-195, 10.1023/A:1021198724250, 2002.

Chen, S. H., Cheng, M. M., Guo, Z., Xu, W., Du, X. H., and Li, Y.: Enhanced atmospheric ammonia (NH3) pollution in China from 2008 to 2016: Evidence from a combination of observations and emissions, Environmental Pollution, 263, ARTN 114421, 10.1016/j.envpol.2020.114421, 2020.

Cong, H., Zhao, L., Wang, J., and Yao, Z.: Current situation and development demand analysis of rural energy in China, Transactions of the Chinese Society of Agricultural Engineering, 33, 224-231, 2017 (in Chinese).

Crippa, M., Solazzo, E., Huang, G. L., Guizzardi, D., Koffi, E., Muntean, M., Schieberle, C., Friedrich, R., and Janssens-Maenhout, G.: High resolution temporal profiles in the Emissions Database for Global Atmospheric Research, Scientific Data, 7, ARTN 121, 10.1038/s41597-020-0462-2, 2020.

Ding, A. J., Huang, X., Nie, W., Sun, J. N., Kerminen, V. M., Petaja, T., Su, H., Cheng, Y. F., Yang, X. Q., Wang, M. H., Chi, X. G., Wang, J. P., Virkkula, A., Guo, W. D., Yuan, J., Wang, S. Y., Zhang, R. J., Wu, Y. F., Song, Y., Zhu, T., Zilitinkevich, S., Kulmala, M., and Fu, C. B.: Enhanced haze pollution by black carbon in megacities in China, Geophysical Research Letters, 43, 2873-2879, 10.1002/2016gl067745, 2016.

Dong, Y., Chen, C., Huang, C., Wang, H., Li, L., Dai, P., and Jia, J.: Anthropogenic emissions and distribution of ammonia over the Yangtze River Delta, Acta Scientiae Circumstantiae, 29, 1611-1617, 2009.

European Environment Agency (EEA): EMEP/CORINAIR Air Pollutant Emission Inventory Guidebook-2019, 3.B Manure management, available at: https://www.eea.europa.eu/publications/emep-eea-guidebook-2019/part-b-sectoral-guidance-chapters/4-agriculture/, (last: 25 May 2021), 2019.

Elser, M., Huang, R. J., Wolf, R., Slowik, J. G., Wang, Q. Y., Canonaco, F., Li, G. H., Bozzetti, C., Daellenbach, K. R., Huang, Y., Zhang, R. J., Li, Z. Q., Cao, J. J., Baltensperger, U., El-Haddad, I., and Prevot, A. S. H.: New insights into PM2.5 chemical composition and sources in two major cities in China during extreme haze events using aerosol mass spectrometry, Atmos Chem Phys, 16, 3207-3225, 10.5194/acp-16-3207-2016, 2016.

Fu, X., Wang, S., Xing, J., Zhang, X., Wang, T., and Hao, J.: Increasing Ammonia Concentrations Reduce the Effectiveness of Particle Pollution Control Achieved via SO_2 and NO_X Emissions Reduction in East China, Environmental Science &

https://doi.org/10.5194/acp-2021-439
Preprint. Discussion started: 18 June 2021
© Author(s) 2021. CC BY 4.0 License.

Technology Letters, 4, 221-227, 10.1021/acs.estlett.7b00143, 2017.

Fu, X., Wang, S. X., Ran, L. M., Pleim, J. E., Cooter, E., Bash, J. O., Benson, V., and Hao, J. M.: Estimating NH3 emissions from agricultural fertilizer application in China using the bi-directional CMAQ model coupled to an agro-ecosystem model, Atmos Chem Phys, 15, 6637-6649, 10.5194/acp-15-6637-2015, 2015.

Han, X., Zhu, L. Y., Liu, M. X., Song, Y., and Zhang, M. G.: Numerical analysis of agricultural emissions impacts on PM2.5 in China using a high-resolution ammonia emission inventory, Atmos Chem Phys, 20, 9979-9996, 10.5194/acp-20-9979-2020, 2020.

Hu, Y., Cheng, H., and Tao, S.: Environmental and human health challenges of industrial livestock and poultry farming in China and their mitigation, Environment International, 107, 111-130, https://doi.org/10.1016/j.envint.2017.07.003, 2017.

Huang, X., Song, Y., Li, M. M., Li, J. F., Huo, Q., Cai, X. H., Zhu, T., Hu, M., and Zhang, H. S.: A high-resolution ammonia emission inventory in China, Global Biogeochemical Cycles, 26, Artn Gb1030, 10.1029/2011gb004161, 2012.

Kang, Y. N., Liu, M. X., Song, Y., Huang, X., Yao, H., Cai, X. H., Zhang, H. S., Kang, L., Liu, X. J., Yan, X. Y., He, H., Zhang, Q., Shao, M., and Zhu, T.: High-resolution ammonia emissions inventories in China from 1980 to 2012, Atmos Chem Phys, 16, 2043-2058, 10.5194/acp-16-2043-2016, 2016.

Kong, L., Tang, X., Zhu, J., Wang, Z. F., Pan, Y. P., Wu, H. J., Wu, L., Wu, Q. Z., He, Y. X., Tian, S. L., Xie, Y. Z., Liu, Z. R., Sui, W. X., Han, L. N., and Carmichael, G.: Improved Inversion of Monthly Ammonia Emissions in China Based on the Chinese Ammonia Monitoring Network and Ensemble Kalman Filter, Environmental Science & Technology, 53, 12529-12538, 10.1021/acsest.9b02701, 2019.

Kurokawa, J. and Ohara, T.: Long-term historical trends in air pollutant emissions in Asia: Regional Emission inventory in ASia (REAS) version 3, Atmos. Chem. Phys., 20, 12761-12793, 10.5194/acp-20-12761-2020, 2020.

Li, B., Wang, J., Wu, S., Jia, Z., Li, Y., Wang, T., and Zhou, S.: New Method for Improving Spatial Allocation Accuracy of Industrial Energy Consumption and Implications for Polycyclic Aromatic Hydrocarbon Emissions in China, Environmental Science & Technology, 53, 4326-4334, 10.1021/acs.est.8b06915, 2019a.

Li, B., Zhou, S., Wang, T., Sui, X., Jia, Z., Li, Y., Wang, J., and Wu, S.: An improved gridded polycyclic aromatic hydrocarbon emission inventory for the lower reaches of the Yangtze River Delta region from 2001 to 2015 using satellite data, Journal of hazardous materials, 360, 329-339, 2018.

Li, K., Jacob, D. J., Liao, H., Zhu, J., Shah, V., Shen, L., Bates, K. H., Zhang, Q., and Zhai, S.: A two-pollutant strategy for improving ozone and particulate air quality in China, Nature Geoscience, 12, 906-910, 10.1038/s41561-019-0464-x, 2019b.

Li, M., Liu, H., Geng, G. N., Hong, C. P., Liu, F., Song, Y., Tong, D., Zheng, B., Cui, H. Y., Man, H. Y., Zhang, Q., and He, K. B.: Anthropogenic emission inventories in China: a review, National Science Review, 4, 834-866, 10.1093/nsr/nwx150, 2017.

Liu, L., Zhang, X. Y., Wong, A. Y. H., Xu, W., Liu, X. J., Li, Y., Mi, H., Lu, X. H., Zhao, L. M., Wang, Z., Wu, X. D., and Wei, J.: Estimating global surface ammonia concentrations inferred from satellite retrievals, Atmos Chem Phys, 19, 12051-

https://doi.org/10.5194/acp-2021-439
Preprint. Discussion started: 18 June 2021
© Author(s) 2021. CC BY 4.0 License.

12066, 10.5194/acp-19-12051-2019, 2019a.

Liu, M. X., Huang, X., Song, Y., Tang, J., Cao, J. J., Zhang, X. Y., Zhang, Q., Wang, S. X., Xu, T. T., Kang, L., Cai, X. H., Zhang, H. S., Yang, F. M., Wang, H. B., Yu, J. Z., Lau, A. K. H., He, L. Y., Huang, X. F., Duan, L., Ding, A. J., Xue, L. K., Gao, J., Liu, B., and Zhu, T.: Ammonia emission control in China would mitigate haze pollution and nitrogen deposition, but worsen acid rain, Proceedings of the National Academy of Sciences of the United States of America, 116, 7760-7765, 10.1073/pnas.1814880116, 2019b.

Liu, X. J., Zhang, Y., Han, W. X., Tang, A. H., Shen, J. L., Cui, Z. L., Vitousek, P., Erisman, J. W., Goulding, K., Christie, P., Fangmeier, A., and Zhang, F. S.: Enhanced nitrogen deposition over China, Nature, 494, 459-462, 10.1038/nature11917, 2013.

Ministry of Agriculture and Rural Affairs of China (MARA): China Animal Husbandry and Veterinary Yearbook, 2017 (in Chinese).

Ministry of Environmental Protection (MEP): The Guideline of Emission Inventory Development for Atmospheric Ammonia, 2014 (in Chinese).

Monfreda, C., Ramankutty, N., and Foley, J. A.: Farming the planet: 2. Geographic distribution of crop areas, yields, physiological types, and net primary production in the year 2000, Global Biogeochemical Cycles, 22, https://doi.org/10.1029/2007GB002947, 2008.

National Bureau of Statistics (NBS): China Statistical Yearbook 2016, 2017a (in Chinese).

National Bureau of Statistics (NBS): China Energy Statistical Yearbook 2016, 2017b (in Chinese).

National Bureau of Statistics (NBS): China Statistical Yearbook of Environment 2016, 2017c (in Chinese).

National Bureau of Statistics (NBS): China Industry Statistical Yearbook 2016, 2017d (in Chinese).

National Development and Reform Commission of China (NDRC): National data on the cost and profit of agricultural product 2016, 2017 (in Chinese).

Pan, Y. P., Tian, S. L., Zhao, Y. H., Zhang, L., Zhu, X. Y., Gao, J., Huang, W., Zhou, Y. B., Song, Y., Zhang, Q., and Wang, Y. S.: Identifying Ammonia Hotspots in China Using a National Observation Network, Environmental Science & Technology, 52, 3926-3934, 10.1021/acs.est.7b05235, 2018.

Paulot, F., Jacob, D. J., Pinder, R. W., Bash, J. O., Travis, K., and Henze, D. K.: Ammonia emissions in the United States, European Union, and China derived by high-resolution inversion of ammonium wet deposition data: Interpretation with a new agricultural emissions inventory (MASAGE_NH3), Journal of Geophysical Research-Atmospheres, 119, 4343-4364, 10.1002/2013jd021130, 2014.

Qian, Y., Song, K., Hu, T., and Ying, T.: Environmental status of livestock and poultry sectors in China under current transformation stage, Science of The Total Environment, 622-623, 702-709, https://doi.org/10.1016/j.scitotenv.2017.12.045, 2018.

Qiu, B., Qi, W., Tang, Z., Chen, C., and Wang, X.: Rice cropping density and intensity lessened in southeast China during the twenty-first century, Environmental Monitoring and Assessment, 188, 5, 10.1007/s10661-015-5004-6, 2015.

Qiu, X., Duan, L., Chai, F., Wang, S., Yu, Q., and Wang, S.: Deriving High-Resolution Emission Inventory of Open Biomass Burning in China based on Satellite Observations, Environmental science & technology, 50, 11779-11786, 2016.

Sheppard, L. J., Leith, I. D., Mizunuma, T., Neil Cape, J., Crossley, A., Leeson, S., Sutton, M. A., van Dijk, N., and Fowler, D.: Dry deposition of ammonia gas drives species change faster than wet deposition of ammonium ions: evidence from a long-term field manipulation, 17, 3589-3607, https://doi.org/10.1111/j.1365-2486.2011.02478.x, 2011.

Streets, D. G., Bond, T., Carmichael, G., Fernandes, S., Fu, Q., He, D., Klimont, Z., Nelson, S., Tsai, N., and Wang, M. Q.: An inventory of gaseous and primary aerosol emissions in Asia in the year 2000, Journal of Geophysical Research: Atmospheres, 108, 2003.

Van Damme, M., Whitburn, S., Clarisse, L., Clerbaux, C., Hurtmans, D., and Coheur, P. F.: Version 2 of the IASI NH3 neural network retrieval algorithm: near-real-time and reanalysed datasets, Atmos Meas Tech, 10, 4905-4914, 10.5194/amt-10-4905-2017, 2017.

Van Damme, M., Clarisse, L., Heald, C. L., Hurtmans, D., Ngadi, Y., Clerbaux, C., Dolman, A. J., Erisman, J. W., and Coheur, P. F.: Global distributions, time series and error characterization of atmospheric ammonia (NH3) from IASI satellite observations, Atmos Chem Phys, 14, 2905-2922, 10.5194/acp-14-2905-2014, 2014.

Van Damme, M., Clarisse, L., Dammers, E., Liu, X., Nowak, J. B., Clerbaux, C., Flechard, C. R., Galy-Lacaux, C., Xu, W., Neuman, J. A., Tang, Y. S., Sutton, M. A., Erisman, J. W., and Coheur, P. F.: Towards validation of ammonia (NH3) measurements from the IASI satellite, Atmospheric Measurement Techniques, 8, 1575-1591, 10.5194/amt-8-1575-2015, 2015.

Wang, G. H., Zhang, R. Y., Gomez, M. E., Yang, L. X., Zamora, M. L., Hu, M., Lin, Y., Peng, J. F., Guo, S., Meng, J. J., Li, J. J., Cheng, C. L., Hu, T. F., Ren, Y. Q., Wang, Y. S., Gao, J., Cao, J. J., An, Z. S., Zhou, W. J., Li, G. H., Wang, J. Y., Tian, P. F., Marrero-Ortiz, W., Secrest, J., Du, Z. F., Zheng, J., Shang, D. J., Zeng, L. M., Shao, M., Wang, W. G., Huang, Y., Wang, Y., Zhu, Y. J., Li, Y. X., Hu, J. X., Pan, B., Cai, L., Cheng, Y. T., Ji, Y. M., Zhang, F., Rosenfeld, D., Liss, P. S., Duce, R. A., Kolb, C. E., and Molina, M. J.: Persistent sulfate formation from London Fog to Chinese haze, Proceedings of the National Academy of Sciences of the United States of America, 113, 13630-13635, 10.1073/pnas.1616540113, 2016.

Wang, J., Ma, W., Jiang, R., and Zhang, F.: Analysis about Amount and Ratio of Basal Fertilizer and Topdressing Fertilizer on Rice, Wheat, Maize in China, Chinese Journal of Soil Science, 39, 329-333, 10.19336/j.cnki.trtb.2008.02.024, 2008.

Wang, X., Zou, C., Gao, X., Guan, X., Zhang, Y., Shi, X., and Chen, X.: Nitrate leaching from open-field and greenhouse vegetable systems in China: a meta-analysis, Environmental Science and Pollution Research, 25, 31007-31016, 10.1007/s11356-018-3082-z, 2018.

Wang, Y., Zhang, Q. Q., He, K., Zhang, Q., and Chai, L.: Sulfate-nitrate-ammonium aerosols over China: response to 2000-2015 emission changes of sulfur dioxide, nitrogen oxides, and ammonia, Atmos Chem Phys, 13, 2635-2652, 10.5194/acp-13-2635-2013, 2013.

Warner, J. X., Dickerson, R. R., Wei, Z., Strow, L. L., Wang, Y., and Liang, Q.: Increased atmospheric ammonia over the world's major agricultural areas detected from space, Geophysical Research Letters, 44, 2875-2884, 10.1002/2016gl072305, 2017.

Xia, L., Li, X., Ma, Q., Lam, S. K., Wolf, B., Kiese, R., Butterbach-Bahl, K., Chen, D., Li, Z., and Yan, X.: Simultaneous quantification of N2, NH3 and N2O emissions from a flooded paddy field under different N fertilization regimes, 26, 2292-2303, https://doi.org/10.1111/gcb.14958, 2020.

Xu, P., Koloutsou-Vakakis, S., Rood, M. J., and Luan, S.: Projections of NH_3 emissions from manure generated by livestock production in China to 2030 under six mitigation scenarios, Science of the Total Environment, 607, 78-86, 10.1016/j.scitotenv.2017.06.258, 2017.

Xu, P., Zhang, Y. S., Gong, W. W., Hou, X. K., Kroeze, C., Gao, W., and Luan, S. J.: An inventory of the emission of ammonia from agricultural fertilizer application in China for 2010 and its high-resolution spatial distribution, Atmos Environ, 115, 141-148, 10.1016/j.atmosenv.2015.05.020, 2015.

Xu, P., Liao, Y. J., Lin, Y. H., Zhao, C. X., Yan, C. H., Cao, M. N., Wang, G. S., and Luan, S. J.: High-resolution inventory of ammonia emissions from agricultural fertilizer in China from 1978 to 2008, Atmos Chem Phys, 16, 1207-1218, 10.5194/acp-16-1207-2016, 2016.

You, Y., Kanawade, V. P., de Gouw, J. A., Guenther, A. B., Madronich, S., Sierra-Hernández, M. R., Lawler, M., Smith, J. N., Takahama, S., Ruggeri, G., Koss, A., Olson, K., Baumann, K., Weber, R. J., Nenes, A., Guo, H., Edgerton, E. S., Porcelli, L., Brune, W. H., Goldstein, A. H., and Lee, S. H.: Atmospheric amines and ammonia measured with a chemical ionization mass spectrometer (CIMS), Atmos. Chem. Phys., 14, 12181-12194, 10.5194/acp-14-12181-2014, 2014.

Zhang, F., Chen, X., and Chen, Q.: Fertilization Guide for Major Crops in China, China Agricultural University Press2009.

Zhang, L., Chen, Y. F., Zhao, Y. H., Henze, D. K., Zhu, L. Y., Song, Y., Paulot, F., Liu, X. J., Pan, Y. P., Lin, Y., and Huang, B. X.: Agricultural ammonia emissions in China: reconciling bottom-up and top-down estimates, Atmos Chem Phys, 18, 339-355, 10.5194/acp-18-339-2018, 2018.

Zhang, Q., Zheng, Y., Tong, D., Shao, M., Wang, S., Zhang, Y., Xu, X., Wang, J., He, H., and Liu, W.: Drivers of improved PM2. 5 air quality in China from 2013 to 2017, Proceedings of the National Academy of Sciences, 116, 24463-24469, 2019.

Zhang, W. and Zhang, F.: Report on the development of fertilizer in China, China Agricultural University Press2012.

Zhang, X. M., Wu, Y. Y., Liu, X. J., Reis, S., Jin, J. X., Dragosits, U., Van Damme, M., Clarisse, L., Whitburn, S., Coheur, P. F., and Gu, B. J.: Ammonia Emissions May Be Substantially Underestimated in China, Environmental Science & Technology, 51, 12089-12096, 10.1021/acs.est.7b02171, 2017.

Zhao, B., Wang, S. X., Wang, J. D., Fu, J. S., Liu, T. H., Xu, J. Y., Fu, X., and Hao, J. M.: Impact of national NOx and SO2 control policies on particulate matter pollution in China, Atmos Environ, 77, 453-463, 10.1016/j.atmosenv.2013.05.012, 2013.

Zhao, Y., Nielsen, C. P., Lei, Y., McElroy, M. B., and Hao, J.: Quantifying the uncertainties of a bottom-up emission inventory of anthropogenic atmospheric pollutants in China, Atmos Chem Phys, 11, 2295-2308, 10.5194/acp-11-2295-2011, 2011.

https://doi.org/10.5194/acp-2021-439
Preprint. Discussion started: 18 June 2021
© Author(s) 2021. CC BY 4.0 License.
Atmospheric Chemistry and Physics Discussions

Zhao, Y., Yuan, M. C., Huang, X., Chen, F., and Zhang, J.: Quantification and evaluation of atmospheric ammonia emissions with different methods: a case study for the Yangtze River Delta region, China, Atmos Chem Phys, 20, 4275-4294, 10.5194/acp-20-4275-2020, 2020.

Zheng, B., Tong, D., Li, M., Liu, F., Hong, C., Geng, G., Li, H., Li, X., Peng, L., and Qi, J.: Trends in China's anthropogenic emissions since 2010 as the consequence of clean air actions, Atmos Chem Phys, 18, 14095-14111, 2018.

Zhou, F., Ciais, P., Hayashi, K., Galloway, J., Kim, D. G., Yang, C. L., Li, S. Y., Liu, B., Shang, Z. Y., and Gao, S. S.: Re-estimating NH3 Emissions from Chinese Cropland by a New Nonlinear Model, Environ Sci Technol, 50, 564-572, 10.1021/acs.est.5b03156, 2016.

Zhou, Y., Xing, X., Lang, J., Chen, D., Cheng, S., Lin, W., Xiao, W., and Liu, C.: A comprehensive biomass burning emission inventory with high spatial and temporal resolution in China, Atmos Chem Phys, 17, 2839, 2017.